PROCEEDINGS OF SCIENCE

JUNO status and prospects

Jie Zhao on behalf of the JUNO collaboration[a,*]

[a] *Institute of High Energy Physics, Chinese Academy of Sciences, 19B Yuquan Road, Shijingshan District, Beijing, China*

E-mail: zhaojie@ihep.ac.cn

The Jiangmen Underground Neutrino Observatory (JUNO) collaboration has completed the construction of a 20-kt liquid scintillator detector in a laboratory 700 m (1800 m.w.e.) underground to address many important topics in neutrino and astro-particle physics. Initial testing and performance studies show that key specifications have been mostly met. The detector is clean enough to start the reactor antineutrino oscillation analysis. The energy non-linearity is known to be smaller than 1%. For events in radius smaller than 16 m, the residual energy non-uniformity scanned along the z-axis is smaller than 0.5%. The light yield is larger than 1600 p.e./MeV for ^{68}Ge calibration source located at the centre of the detector, while it is larger than 1800 p.e./MeV for neutrons from the AmBe or AmC calibration sources, which is better than expectations [1]. The energy resolution for α from ^{214}Po is about 3% at 0.92 MeV, while it is about 3.4% at 2×0.511 MeV for ^{68}Ge. We are excited to have started the physics data taking, and the analysis of the first data and the understanding of the detector performance is in progress.

The 17th International Conference on Heavy Quarks and Leptons (HQL 2025)
15-19 September, 2025
Peking University, Beijing, China

*Speaker

PoS(HQL2025)072

1. Introduction

The Jiangmen Underground Neutrino Observatory (JUNO) [2] is located in southern China, approximately 52.5 km from both the Taishan and Yangjiang Nuclear Power Plants. The main detector is situated underground with an overburden of about 700 m. There are two access routes from the surface to the underground experimental hall: a vertical shaft measuring 563 m in depth and a slope tunnel 1,265 m in length with a gradient of 42.5%. Civil construction was completed in December 2021, and the detector was assembled over the following three years. JUNO is a multi-purpose neutrino observatory. It is designed to detect neutrinos from various sources, including nuclear reactors, the atmosphere, and the sun, in order to study neutrino oscillations and their fundamental properties. Additionally, JUNO will be able to observe neutrinos from supernovae and the Earth's interior, contributing to a better understanding of stellar mechanisms and the structure of matter within planetary bodies.

To support its extensive physics program, JUNO requires a carefully designed detector. The primary goal is to determine the neutrino mass ordering by detecting reactor antineutrinos. This objective presents a major challenge: the spectral differences between normal and inverted mass ordering are extremely subtle, demanding exceptionally precise energy spectrum measurements. Therefore, high statistics (10^5 events in 6 years), excellent energy resolution (3% at 1 MeV), minimal spectral shape uncertainty (1%), and low background (3%) are essential.

2. JUNO detector construction

The conceptual design of the JUNO detector [2] is illustrated in the Figure 1. For simplicity and cost efficiency, the detector features a two-layer structure: an acrylic vessel containing the LS, supported by a stainless steel (SS) frame. A total of 17,612 20-inch and 25,600 3-inch PMTs are installed on the SS frame, designed to detect the faint light signals generated by neutrino interactions with the LS. Surrounding the acrylic vessel is an ultrapure water buffer, which serves both as a shielding layer and as a muon veto system via Cherenkov radiation detection. Above the acrylic tank, a top tracker [3] is installed to complement the water Cherenkov detectors in muon identification. In addition, a calibration system is incorporated, which includes a calibration house and a top chimney, allowing calibration sources to be inserted into the detector for periodic performance monitoring and energy scale calibration.

The SS frame was assembled using 120,000 sets of specially designed high-strength rivet bolts, ensuring structural consistency and eliminating the need for welding. As the PMT modules are mounted directly onto this frame, the assembly precision of each grid was controlled to within 3 mm. The final measured radial deviation of the overall structure is –13 mm. The construction of the pillars and the main shell was completed within six months in 2022. Subsequently, the bottom four layers of supporting legs were installed after the completion of the acrylic sphere structure in November 2024.

The 20-kt LS is housed in the acrylic vessel [4], which must meet stringent requirements for high transparency and radiopurity. Due to its enormous size, the vessel could not be manufactured as a single piece. Instead, it was produced in 265 individual segments, each fabricated off-site by the supplier. To ensure surface cleanliness, every panel underwent rigorous treatment including

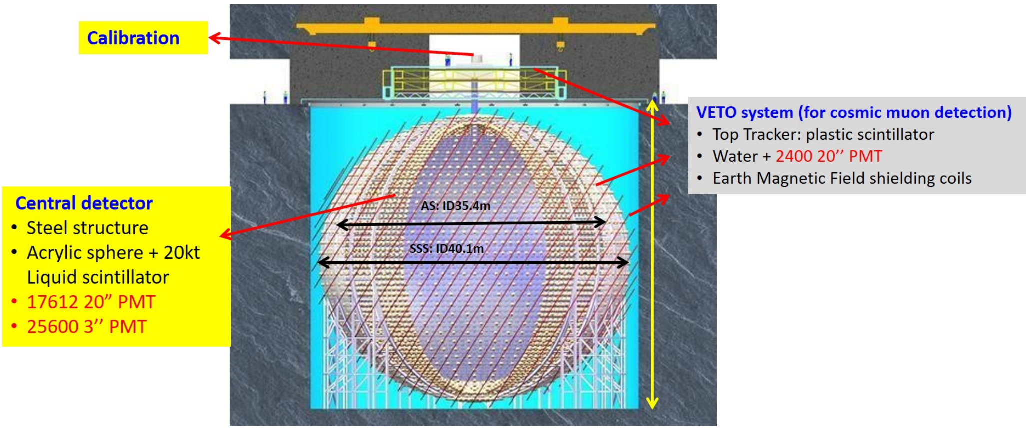

Figure 1: The conceptual design of the JUNO detector.

polishing, sanding, and cleaning, and was then covered with a 50-μm polyethylene (PE) film for protection during transportation to the JUNO site [5]. On-site, all segments were assembled and bonded together inside the experimental hall. The construction involved 21 cyclic operational phases, each taking 20–30 days, with a total bonding length reaching 2 km. Throughout this process, innovative large-volume injection, polymerization, and annealing technologies were developed to facilitate precision assembly. The final fitted diameter deviation of all the survey points around the completed acrylic vessel is –23 mm.

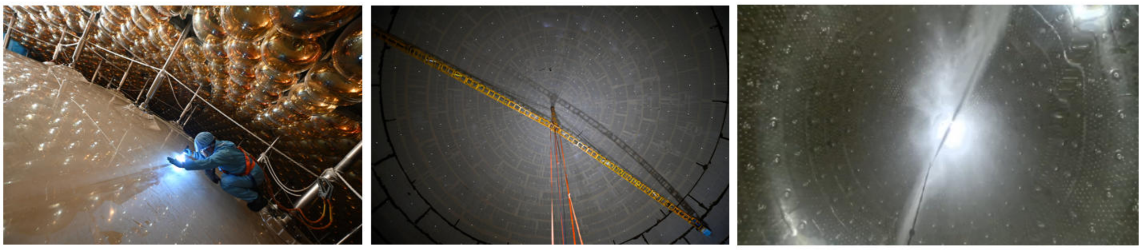

Figure 2: The final inspection of the interior and exterior surfaces of the acrylic vessel are shown in the two left figures, while the right figure illustrates the high-pressure water jet cleaning process.

After the construction of the acrylic vessel, we have a final checks of its inside and outside, as shown in the two left figures of Figure 2. In order to improve the cleanliness inside the vessel, we have a moisture spray over two days to reduce dust levels inside the vessel air from class 10,000 to 100 level. Then we took two weeks high pressure water jet to remove the protection film and clean the inner surface by 3D rotating nozzle, as shown in the right figure of Figure 2. Then we check the water cleanliness reached Level 50 standard (MIL-STD-1246C).

All PMTs underwent comprehensive testing and were encapsulated with waterproof potting. Based on test results, the average photon detection efficiency (PDE) reached 28.5% for dynode PMTs and 30.1% for microchannel-plate (MCP) PMTs; detailed performance data can be found in Ref [6, 7]. Each 20-inch PMT is equipped with an acrylic cover on the top and a SS cover at the bottom to prevent chain explosions triggered by individual tube failures. A hybrid detection system incorporating both 20-inch and 3-inch PMTs was deployed to achieve optimal energy resolution and charge linearity. The assembly precision was maintained within 1 mm. Due to minor deformations encountered during detector installation, 17 of the 20-inch PMTs and 13 of the 3-inch PMTs could not be installed as originally planned.

To enhance the signal-to-noise ratio and achieve superior energy resolution, custom underwater electronics were developed. The waterproof housing for these electronics was tested at a depth of 40 meters to verify its performance and reliability under high-pressure conditions. Each underwater electronics unit is connected to three 20-inch PMTs, while a single unit supports readout for 128 3-inch PMTs.

The final external and internal views of the completed detector are shown in Figure 3.

Figure 3: The final external (left) and internal (right) views of the completed detector.

3. Detector filling

The filling process was conducted in two stages. The first stage involved the simultaneous filling of ultrapure water both inside and outside the acrylic sphere. Throughout this process, the liquid and air pressures were carefully balanced on both sides of the acrylic tank to ensure structural safety. Due to diurnal temperature fluctuations, which induced periodic pressure variations, and the need for gas exchange in both the water pipes and the acrylic vessel, high-purity nitrogen was used for ventilation to minimize the introduction of radioactive gases from the air. The structural stress of the detector was continuously monitored and remained consistent with design expectations. A total of 60 kt of ultrapure water was filled over a period of 45 days, starting on December 18, 2024. The water temperature was maintained uniformly at (21.1±)°C. The measured attenuation length exceeded 60 m, and radiopurity levels were better than required, with U/Th concentrations below 0.4×10^{-15} g/g, ^{222}Rn activity below 5 mBq/m^3, and ^{226}Ra below 10 μBq/m^3. The muon tagging efficiency reached 99.99%.

The second stage of the filling process involved replacing the water inside the acrylic vessel with LS. To ensure the radiopurity and optical transparency of the 20-kt LS, the filling system incorporated four purification plants (using Al_2O_3 columns, distillation, water extraction, and gas stripping), one LS mixing plant, and dedicated facilities for producing high-purity nitrogen and water. Throughout the filling process, LS samples from each production system were analyzed weekly using ICP-MS to screen for uranium and thorium contamination, maintaining levels below 1×10^{-16} g/g [8]. The ^{222}Rn concentration in the central detector was continuously monitored; fresh

LS consistently exhibited ^{222}Rn concentrations below 1 mBq/m³. During periods when filling was paused, the ^{222}Rn leak rate was measured to be less than 0.5 mBq/h. The attenuation length of the LS was also tracked during filling. The weighted average attenuation length exceeded 20 m, meeting the required optical specifications.

The detector completed the LS filling on August 22, 2025. Subsequently, an additional half-day operation was conducted to replace 100 t of older LS from the bottom of the vessel. This was followed by a two-day comprehensive detector calibration. Data acquisition officially commenced at 8:00 on August 26, 2025.

4. Preliminary detector performance

Based on data analysis, the event rate within the energy range of 0.7–6 MeV and within a radial distance of R<17.2 m is less than 7 Hz. This meets the design target of 7.2 Hz [9] and is fully sufficient for reactor antineutrino analysis. The ^{238}U concentration, as determined from Bi–Po events in a small fiducial volume with low radon background, reached 3×10^{-17} g/g. In contrast, the global fit to radon decay across the full detector yielded a plateau value of 10^{-16} g/g. The measured concentration of ^{232}Th in the volume with R<13 m is below 10^{-16} g/g. The total ^{210}Po activity in the LS is less than 10^5 cpd/kt.

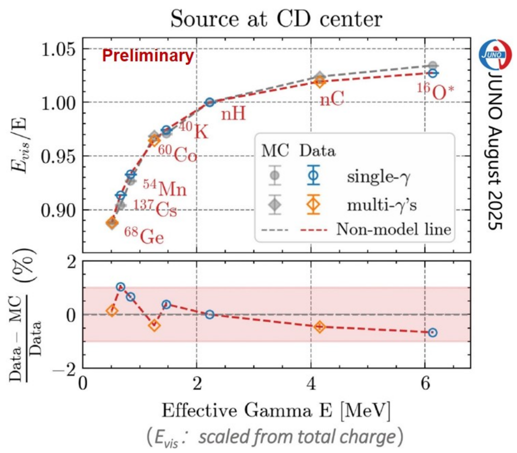

Figure 4: Comparison of non-linearity in central detector LS between data and simulation.

We have developed comprehensive 1D, 2D, and 3D calibration scanning systems utilizing laser, e^+, γ, and neutron sources, as well as neutron/α background events for detector calibration [10]. Preliminary results of the energy non-linearity obtained from the calibration are presented in Figure 4. The discrepancy between the experimental data and simulation is less than 1%.

For the volume within R<16 m, the residual energy non-uniformity along the Z-axis is less than 0.5%, as shown in the left Figure 5. The measured light yield exceeds 1600 p.e./MeV for ^{68}Ge events and 1800 p.e./MeV for neutron captures, shown in the right Figure 5, both surpassing initial expectations [1]. The observed difference in light yield between ^{68}Ge and neutron sources is attributed to energy non-linearity effects. While edge-related systematic effects remain under study, further calibration data and software refinements are ongoing to improve spatial response modeling.

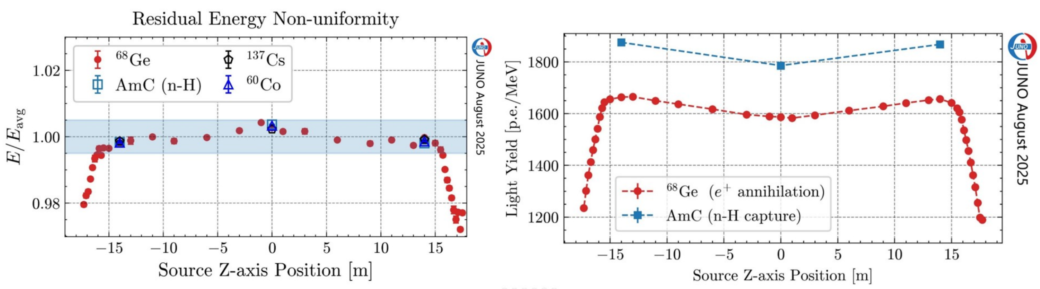

Figure 5: The left figure is the residual energy non-uniformity along the Z-axis within R<16 m. The right figure is light yield of both ^{68}Ge and neutron sources.

The energy resolution for alpha particles from ^{214}Po is approximately 3% at 0.92 MeV, as shown in the left Figure 6. For ^{68}Ge (right Figure 6), the measured energy resolution is about 3.4% at the combined energy of 2×0.511 MeV, which is close to—though slightly worse than—the design target of 3.1%. Further improvements are anticipated with additional calibration data, enhanced noise and flasher event removal, and ongoing refinements in reconstruction and fitting algorithms.

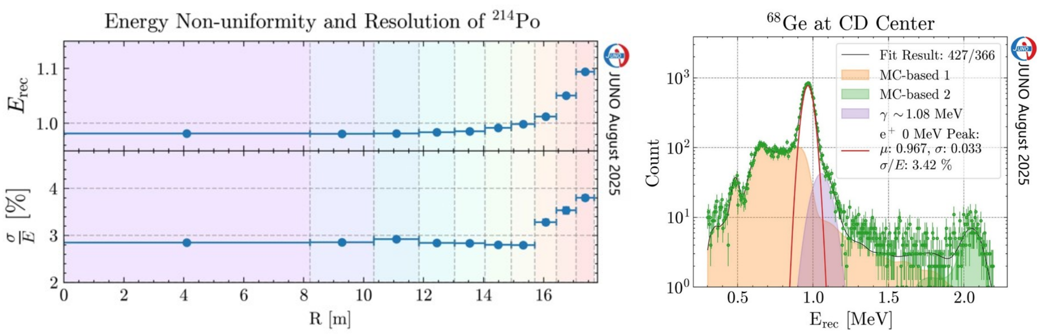

Figure 6: The energy resolution in the detector for alpha (left) and ^{68}Ge (right) sources.

5. Summary

After 17 years—from conceptualization to construction—the JUNO detector has been fully completed, overcoming numerous challenges along the way. Initial testing and performance studies indicate that most key specifications have been successfully achieved. The expected sensitivities for various physics targets are provided in Ref. [2, 11]. We are thrilled to have begun physics data acquisition, and anticipate that the first results from reactor and astrophysical neutrino analyses will be available in the near future.

Acknowledgements

This work is supported by the Youth Innovation Promotion Association of the Chinese Academy of Sciences, CAS Project for Young Scientists in Basic Research (YSBR-099).

References

[1] Angel Abusleme et al. Prediction of Energy Resolution in the JUNO Experiment. *Chin. Phys. C*, 49(1):013003, 2025.

[2] Angel Abusleme et al. JUNO physics and detector. *Prog. Part. Nucl. Phys.*, 123:103927, 2022.

[3] Angel Abusleme et al. The JUNO experiment Top Tracker. *Nucl. Instrum. Meth. A*, 1057:168680, 2023.

[4] Angel Abusleme et al. The design and technology development of the JUNO central detector. *Eur. Phys. J. Plus*, 139(12):1128, 2024.

[5] Yuanxia Li et al. Study on U/Th residual radioactivity in acrylic from surface treatment. *JINST*, 18(05):P05023, 2023.

[6] Angel Abusleme et al. Mass testing and characterization of 20-inch PMTs for JUNO. *Eur. Phys. J. C*, 82(12):1168, 2022.

[7] Chuanya Cao et al. Mass production and characterization of 3-inch PMTs for the JUNO experiment. *Nucl. Instrum. Meth. A*, 1005:165347, 2021.

[8] Yuanxia Li, Jie Zhao, Yayun Ding, Tao Hu, Jiaxuan Ye, Jian Fang, and Liangjian Wen. A practical approach of measuring 238U and 232Th in liquid scintillator to sub-ppq level using ICP-MS. *Radiat. Phys. Chem.*, 230:112579, 2025.

[9] Angel Abusleme et al. Radioactivity control strategy for the JUNO detector. *JHEP*, 11:102, 2021.

[10] Angel Abusleme et al. Calibration Strategy of the JUNO Experiment. *JHEP*, 03:004, 2021.

[11] Angel Abusleme et al. JUNO Sensitivity on Proton Decay $p \to \bar{\nu} K^+$ Searches. *Chin. Phys. C*, 47(11):113002, 2023.